

Possibility of direct Mott insulator-to-superfluid transitions in weakly disordered boson systems

Sung Yong Park and Ji-Woo Lee

Department of Physics and Center for Theoretical Physics, Seoul National University, Seoul 151-742, Korea

Min-Chul Cha

Department of Physics, Hanyang University, Kyunggi-do, Ansan 425-791, Korea

M. Y. Choi, B. J. Kim,* and Doochul Kim

Department of Physics and Center for Theoretical Physics, Seoul National University, Seoul 151-742, Korea

(Received 10 November 1998)

We study the zero-temperature phase transitions of a two-dimensional disordered boson Hubbard model at incommensurate boson densities. Via matrix diagonalization and quantum Monte Carlo simulations, we construct the phase diagram and evaluate the correlation length exponent ν . In the presence of weak disorder, we obtain $\nu=0.5\pm 0.1$, the same value as that in the pure model, near the tip of a Mott insulator lobe, using the dynamical critical exponent $z=2$. As the strength of disorder is increased beyond a certain value, however, the value of ν is found to change to 0.9 ± 0.1 . This result strongly suggests that there exist direct Mott insulator-to-superfluid transitions around the tip of a Mott insulator lobe in the weak disorder regime.

[S0163-1829(99)08513-6]

Two-dimensional (2D) interacting boson systems display quantum phase transitions¹ from an insulating state to a superfluid (SF) state at zero temperature. Physical realization of this transition may include disordered thin-film superconductors, Josephson-junction arrays, granular superconductors,² and ⁴He films adsorbed in porous media.³ In the absence of disorder the insulating state is a Mott insulator (MI), which has a commensurate value of the boson density since, otherwise, excessive bosons or holes will move freely to yield a superfluid. The excessive bosons or holes can be localized, on the other hand, in the presence of disorder, to make an incommensurate insulator. The resulting Bose glass (BG) insulating phase has attracted considerable interest recently. In the mean-field theory,⁴ it has been argued that in the presence of disorder the transition from a Mott insulator to a superfluid occurs only through the BG phase. However, a recent quantum Monte Carlo study,⁵ performed at the tip of an MI lobe (i.e., at a commensurate value of the boson density), has demonstrated the existence of a direct MI-SF transition. The subsequent renormalization group study⁶ has been interpreted to suggest that the direct MI-SF transition occurs around the tip of the MI lobe in high dimensions ($d > 4$) but only at the tip in lower dimensions ($2 \leq d < 4$). These results raise an interesting question as to whether such a direct MI-SF transition occurs even at incommensurate values of the boson density.

This paper investigates the possibility of the direct MI-SF transition off the tip of an MI lobe in two dimensions. We perform both matrix diagonalization and quantum Monte Carlo simulations, and find evidences for the direct transition around the tip of an MI lobe in the weak disorder limit. The superfluid onset points are identified and the correlation length critical exponents are estimated at various disorder strengths. The corresponding phase diagram for weak disorder is constructed.

We consider the boson Hubbard model with disorder, described by the Hamiltonian

$$H = \frac{U}{2} \sum_i n_i^2 - \sum_i (\mu + v_i) n_i - t \sum_{\langle i,j \rangle} (b_i^\dagger b_j + b_i b_j^\dagger), \quad (1)$$

where b_i^\dagger and b_i are the boson creation and destruction operators at site i on an $L \times L$ square lattice, and $n_i \equiv b_i^\dagger b_i$ is the number operator. In Eq. (1), U is the strength of the on-site repulsion, μ is the chemical potential, v_i is the random on-site potential distributed uniformly between $-\Delta$ and Δ , and t measures the hopping strength between nearest-neighbor sites. In the limit of the large number of particles, we may take the phase-only approximation⁷ and reduce Eq. (1) to the quantum phase Hamiltonian

$$H = \frac{U}{2} \sum_i n_i^2 - \sum_i (\mu + v_i) n_i - t \sum_{\langle i,j \rangle} \cos(\phi_i - \phi_j), \quad (2)$$

where ϕ_i is the phase of the bosons condensed at site i and satisfies the relation $[n_i, \phi_j] = i \delta_{ij}$. Note that in this representation, n_i denotes the deviation from the mean-integer number n_0 (around the mean number $\langle b_i^\dagger b_i \rangle$).

In order to determine the phase boundary, we first use the matrix diagonalization method with a truncated basis set. The zero-temperature phase boundary between the MI phase and the SF/BG phase is determined by comparing the ground-state energy of the system at commensurate boson density and that of the system containing an extra hole or particle. The basis set is chosen to include the lowest-energy states of the Hamiltonian given by the first and the second term in Eq. (2) (i.e., the zeroth order in t) and the states coupled to these by hopping up to $(2n+1)$ th order in t , where we set $n=1$ in this paper. We identify the lowest-energy state among the states of which the total boson number is zero as the MI state and the lowest one among the

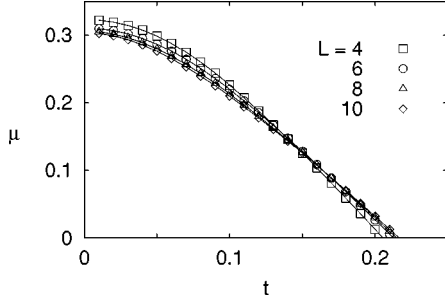


FIG. 1. Phase diagram in the (t, μ) plane for the disorder strength $\Delta = 0.2$. Each line gives an estimate of the phase boundary between the MI state and the SF or BG state, as determined by matrix diagonalization.

states with the total boson number being unity as the SF/BG state, and determine the phase boundary by locating the values of μ (> 0) and t at which the energies of the two states become equal.

Since the basis set includes those states coupled up to the third order in t , the result will be the same as that from the energy perturbation to the same order. The numbers of states involved in this calculation are $4L^4 - 9L^2$ and $4L^2 + 1$ in the cases of the BG/SF state and of the MI state, respectively. We adopt the Lanczos method¹¹ to obtain the lowest eigenvalue and the corresponding eigenstate, and take 2000 disorder realizations for each system size. In the pure case ($\Delta = 0$), we find the phase diagram, which is consistent with the previous perturbation result of Freericks and Monien.¹⁰

Figure 1 shows the zero-temperature phase diagram with the disorder strength $\Delta = 0.2$ up to the system size $L = 10$ obtained from the truncated basis set. The shape of the MI lobe constructed from the previous perturbation result in the pure case¹⁰ should be round and shorter than that obtained here. In the absence of hopping ($t = 0$), where no SF state is possible, the phase boundary (between the MI and BG states) approaches, as the system size L is increased, $0.5 - \Delta$, as it should.

To distinguish the SF phase from the BG phase, we use localization argument, and define the participation ratio as

$$p_L = \left[\frac{\left(\sum_i p_i^2 \right)^2}{\sum_i p_i^4} \right]_{av}, \quad (3)$$

where p_i is the probability that particles are found at site i ,⁵ and $[\dots]_{av}$ denotes the average over different disorder realizations. At the generic SF-BG transition, the participation ratio satisfies the scaling relation

$$\frac{p_L}{L^2} = L^{-y} \tilde{p}(\delta_t L^{1/\nu}), \quad (4)$$

where $\delta_t = (t - t_c)/t_c$ is the distance from the critical point t_c and ν is the correlation length exponent. Here the scaling function \tilde{p} and an additional exponent y have been introduced.^{5,12} Note that since we just consider the states in which the total number of bosons is unity, this method is

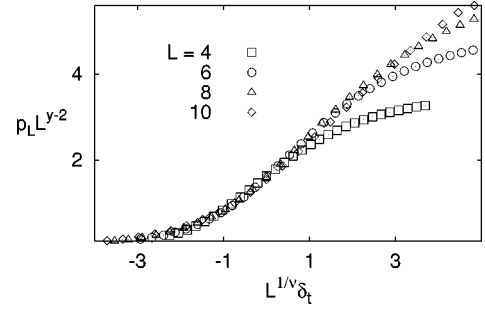


FIG. 2. Scaling plot of the participation ratio p_L near the MI-SF/BG phase boundary, which yields $t_c = 0.12$, $y = 0.92$, and $\nu = 1.5$.

useful to determine the critical point very close to the MI phase, i.e., on the phase boundary in Fig. 1.

Figure 2 presents the finite-size scaling of the participation ratio of the SF/BG state. From this scaling behavior, we obtain $y = 0.92 \pm 0.03$, $\nu = 1.5 \pm 0.3$, and $t_c = 0.12 \pm 0.02$; the latter separates the SF state from the BG one as t (or μ) is varied along the phase boundary in Fig. 1. Accordingly, the system undergoes a direct MI-SF transition as the phase boundary is crossed for small μ (≤ 0.18 in Fig. 1), i.e., near the tip of an MI lobe. Note that the possible origin of this direct MI-SF transition, as discussed later, is the abundance of particle-hole excitations around the tip of a lobe. This suggests that the size of the basis set including the states up to the third order in t might not be sufficient to determine the phase boundary unambiguously and to compute the corresponding exponents accurately. Such abundance of particle-hole excitations is expected to forbid the perturbation calculation to be accurate, possibly causing the discrepancy between the perturbative results¹⁰ and the quantum Monte Carlo results⁸ in the pure case without disorder.

It is thus needed to investigate the transition via quantum Monte Carlo simulations, which are in general more reliable. For that purpose, we follow the standard procedure^{8,9} to transform the 2D quantum phase Hamiltonian in Eq. (2) to the (2+1)-dimensional classical action

$$S = \frac{1}{K} \sum_{(i,t)}^{\nabla \cdot \mathbf{J} = 0} \left[\frac{1}{2} \mathbf{J}_{(i,t)}^2 - (\mu + v_i) J_{(i,t)}^T \right], \quad (5)$$

where the integer current vector $\mathbf{J}_{(i,t)} = (J_{(i,t)}^x, J_{(i,t)}^y, J_{(i,t)}^T)$ is divergenceless on each lattice site (i, t) as indicated. The coupling constant K , corresponding roughly to $\sqrt{t/U}$, takes the role of the temperature.

We perform quantum Monte Carlo simulations on the classical action in Eq. (5), employing the heat bath algorithm⁹ at a classical temperature K . An important quantity in the analysis is the zero-frequency superfluid stiffness

$$\rho = \frac{1}{L_\tau} [\langle n_x^2 \rangle]_{av}, \quad (6)$$

where $n_x = (1/L) \sum_{(i,t)} J_{(i,t)}^x$ is the winding number along the (spatial) x direction. The finite-size scaling behavior of the superfluid stiffness^{9,13} reads

$$\rho = L^{-(d+z-2)} \tilde{\rho}(L^{1/\nu} \delta_t, L_\tau / L^z), \quad (7)$$

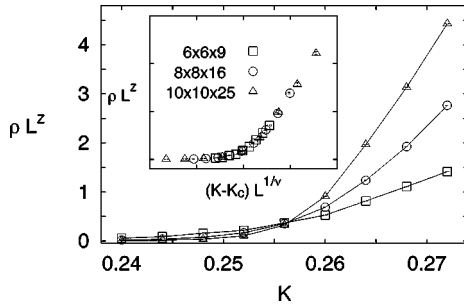


FIG. 3. Behavior of the stiffness ρ for $\mu=0.3$ and $\Delta=0.1$, with the aspect ratio kept constant for $z=2$. The inset shows a scaling plot with $K_c=0.257$ and $\nu=0.5$.

where $\delta=(K-K_c)/K_c$ is the distance from the critical point K_c , the spatial dimension d is two in this paper, and z is the dynamical critical exponent.

In order to investigate the scaling behavior, the value of z should be known in advance. At the very tip of an MI lobe, the direct MI-SF transition in the presence of weak disorder shows the same behavior as the pure system: the dynamical critical exponent $z=1$ and the correlation exponent $\nu=0.67$.⁵ Off the tip, we expect the dynamical exponent $z=2$ in the disordered system since the compressibility is finite at the transition point;⁴ the same number is expected even in the pure case. We, thus, set the dynamical exponent $z=2$, and measure the correlation length exponent ν , the value of which was estimated in the previous studies to be 0.9 ± 0.1 in the BG-SF transition^{5,9} and 0.5 ± 0.1 in the MI-SF transition.^{4,8}

Keeping L_τ/L^z constant, we simulate the systems of sizes $L\times L\times L_\tau=6\times 6\times 9$, $8\times 8\times 16$, and $10\times 10\times 25$. To tune the transition, we vary the temperature K while fixing μ and Δ . We further take the average over 60–200 disorder realizations and, for each disorder realization, perform typically 4000–80000 Monte Carlo sweeps for equilibration, followed by equally many sweeps for measurement. The equilibration is checked through the use of the standard equilibration test technique.^{9,14}

In Fig. 3, we show the results with $z=2$ at $\mu=0.3$ and $\Delta=0.1$. One can identify clearly the common crossing point of $L^z\rho$ at $K_c=0.257\pm 0.003$ as the critical point. The inset of Fig. 3 shows a scaling plot, which yields $\nu=0.5\pm 0.1$, the same value as the pure model.⁴ On the other hand, in the strong-disorder case ($\Delta=0.3$) shown in Fig. 4, the scaling behavior yields $\nu=0.9\pm 0.1$, which agrees well with the pre-

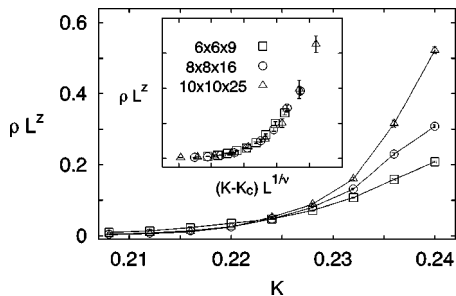


FIG. 4. Behavior of the stiffness ρ for $\mu=0.3$ and $\Delta=0.3$, with the aspect ratio kept constant for $z=2$. The inset shows a scaling plot with $K_c=0.223$ and $\nu=0.9$.

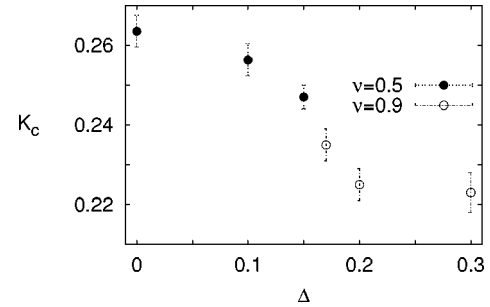


FIG. 5. Critical point K_c as a function of the disorder strength Δ for $\mu=0.3$. The solid dots indicate the direct MI-SF transition points and the open dots the BG-SF transition points.

vious results of the BG-SF transition.^{4,5,9} These demonstrate that in the weak disorder regime a direct MI-SF transition takes place not only at the tip but also off the tip of the MI lobe. Figure 5 presents the critical temperature K_c as a function of the disorder strength Δ for $\mu=0.3$, displaying the direct MI-SF transition occurring for $\Delta<0.16$. It is of interest that the point on which the value of the correlation length exponent ν changes appears to have the maximum slope on the K_c - Δ curve.

Figure 6 summarizes the phase diagram of the disordered boson Hubbard model at the disorder strength $\Delta=0.2$. The phase boundary between the MI and the BG phases is estimated by means of the matrix diagonalization in the system of size $L=10$. Here, we have used the results in Refs. 5 and 10 to scale K as a function of t , which is valid only for small t .

Finally, we discuss the possible origin of the direct MI-SF transition around the tip of an MI lobe. One might think that off the tip the BG phase intervenes very slimly between the MI and SF phases and that our results supporting the direct MI-SF transition merely reflect finite-size effects. Be this the case, the localization length would be large near the tip and the BG phase would manifest itself only on the length scale exceeding the system size. Then, as pointed out in Ref. 6, an anomalous behavior is expected to occur to change the correlation exponent ν , suggesting continuous change of the exponent with the thickness of the BG phase near the tip. On the other hand, our results in Figs. 5 and 6 indicate that the exponent changes quite abruptly, making the above scenario rather unlikely. Near the tip, the particle-hole excitations are

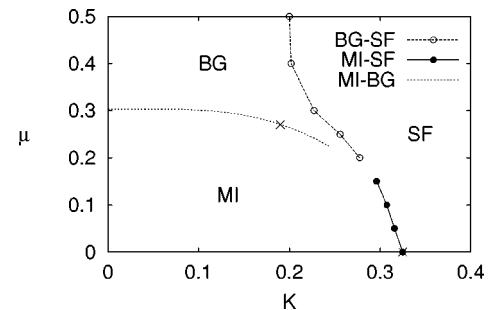


FIG. 6. Phase diagram in the (K, μ) plane for $\Delta=0.2$. The dotted line (without symbols) corresponds to the rescaled data from the matrix diagonalization method, while the solid and dashed lines (with symbols) are the results of quantum Monte Carlo simulations. The two points marked by crosses represent the results in Ref. 5.

ubiquitous and presumably tend to suppress the disorder effects, allowing the possibility of an extended state for the extra boson. Thus the resulting direct MI-SF transition around the tip may reflect the peculiar nature of boson localization.

In summary, we have studied the disordered boson Hubbard model by means of the matrix diagonalization with restricted basis states, which include those states overlapping with each other through nearest-neighbor hopping up to the third order. The finite-size scaling of the participation ratio at $\Delta = 0.2$ gives evidence for the direct MI-SF transition at an incommensurate value of the boson density. To investigate this direct transition more clearly, we have investigated the scaling behavior of the superfluid stiffness via quantum

Monte Carlo simulations and found that as the disorder strength is varied, the value of the correlation exponent ν changes rather abruptly from the weak disorder value 0.5 to the strong disorder one 0.9. This indicates that the direct MI-SF transition occurs for weak disorder at an incommensurate density. The possible origin of this transition could be the abundance of the particle-hole excitations around the tip of an MI lobe, which suggests the peculiar nature of boson localization.

S.Y.P. would like to thank H. Rieger, G. G. Batrouni, and J. Kisker for helpful discussions. This work was supported in part by the Korea Research Foundation made in the program year of 1998 and by the KOSEF through the SRC Program.

*Present address: Department of Theoretical Physics, Umeå University, S-901 87 Umeå, Sweden.

¹S.L. Sondhi, S.M. Girvin, J.P. Carini, and D. Shahar, *Rev. Mod. Phys.* **69**, 315 (1997).

²Y. Liu *et al.*, *Phys. Rev. Lett.* **67**, 2068 (1991); M.A. Paalanen, A.F. Hebard, and R.R. Ruel, *ibid.* **69**, 1604 (1992).

³P.A. Crowell, F.W. van Keuk, and J.D. Reppy, *Phys. Rev. Lett.* **75**, 1106 (1995); P.A. Crowell *et al.*, *Phys. Rev. B* **51**, 12 721 (1995).

⁴M.P.A. Fisher, P.B. Weichman, G. Grinstein, and D.S. Fisher, *Phys. Rev. B* **40**, 546 (1989).

⁵J. Kisker and H. Rieger, *Phys. Rev. B* **55**, R11 981 (1997); *Physica A* **246**, 348 (1997).

⁶F. Pázmándi and G. T. Zimányi, *Phys. Rev. B* **57**, 5044 (1998); I. F. Herbut, *ibid.* **57**, 13 729 (1998).

⁷M.P.A. Fisher and G. Grinstein, *Phys. Rev. Lett.* **60**, 208 (1988).

⁸A. van Otterlo *et al.*, *Phys. Rev. B* **52**, 16 176 (1995).

⁹E.S. Sørensen, M. Wallin, S.M. Girvin, and A.P. Young, *Phys. Rev. Lett.* **69**, 828 (1992); M. Wallin, E.S. Sørensen, S.M. Girvin, and A.P. Young, *Phys. Rev. B* **49**, 12 115 (1994).

¹⁰J.K. Freericks and H. Monien, *Phys. Rev. B* **53**, 2691 (1996).

¹¹C. Lanczos, *J. Res. Natl. Bur. Stand.* **45**, 255 (1950).

¹²F. Pázmándi, G.T. Zimányi, and R. Scalettar, *Phys. Rev. Lett.* **75**, 1356 (1995).

¹³M.-C. Cha, M.P.A. Fisher, S.M. Girvin, M. Wallin, and A.P. Young, *Phys. Rev. B* **44**, 6883 (1991).

¹⁴R.N. Bhatt and A.P. Young, *Phys. Rev. B* **37**, 5606 (1988).